4-1-2004

Scaling Laws for Single and Multiple Electron Loss from Projectiles in Collisions with a Many-electron Target

Antonio C. Santos
Missouri University of Science and Technology

Robert D. DuBois
Missouri University of Science and Technology, dubois@mst.edu

Recommended Citation
A. C. Santos and R. D. DuBois, "Scaling Laws for Single and Multiple Electron Loss from Projectiles in Collisions with a Many-electron Target," *Physical Review A*, American Physical Society (APS), Apr 2004.
The definitive version is available at https://doi.org/10.1103/PhysRevA.69.042709

Scaling laws for single and multiple electron loss from projectiles in collisions with a many-electron target

A. C. F. Santos and R. D. DuBois
University of Missouri–Rolla, Rolla, Missouri 65409, USA
(Received 25 November 2003; published 9 April 2004)

Using measured cross sections, empirical scaling laws are extracted for projectile stripping induced by collisions with a many-electron target. By scaling both the cross sections and the impact velocities, it is shown that a single universal curve can be used to fit data for single and multiple electron loss from negative ions, neutral particles, and singly or multiply charged positive ions. The scaling applies to projectiles ranging from hydrogen to uranium and collision energies ranging from below keV/u to hundreds of MeV/u. At high energies, existing data are consistent with a v^{-1} impact velocity dependence for scaled velocities less than 10. Limited data imply that above 10 the velocity dependence becomes v^{-2}. Using our universal curve, cross sections are predicted for electron loss from low-charge-state heavy ions at 20 and 100 MeV/u.

DOI: 10.1103/PhysRevA.69.042709 PACS number(s): 34.50.Fa, 34.50.Bw, 29.27.Eg

I. INTRODUCTION AND BACKGROUND

Electron loss, also referred to as projectile stripping, has been studied for decades in order to understand fundamental atomic processes. Of particular interest are one- and many-electron processes induced by interactions between two partially screened target nuclei and their bound electrons. Projectile stripping has also been studied to establish design parameters used in accelerating particles to high energies or for limiting beam transport losses and losses in storage rings. Large amounts of information exist, but how the various pieces of data fit together or can be used to extrapolate to arbitrary systems has been explored only for specific cases or over limited regimes. Scaling laws applicable to a wide range of systems are lacking. This is especially true for many-electron collision systems where multielectron processes can dominate and one-electron theories are inadequate.

Recently, large projects in the United States and Germany have caused a renewed interest into the subject of projectile stripping. In the USA it has been proposed to use intense beams of high-energy (10–20 MeV/u) heavy ions to induce laboratory fusion (see Ref. [1]). To achieve the tight focus needed to maintain a high energy density on target, low-charge-state beams must be used. Therefore electron loss by these beams in the reaction chamber must be minimized. In addition, loss processes during the acceleration and transport phases are detrimental and must be minimized. In Germany, an upgrade of the accelerators at GSI-Darmstadt (see Ref. [2]) to provide intense high-energy (tens to hundreds of MeV/u) beams of low-charge-state heavy ions is faced with similar problems. Again, acceleration and transport losses must be minimized. Also, storage lifetimes must be maximized. Required for design parameters is knowledge about total, single, and multiple cross sections for electron loss from low-charge-state ions traveling at high energies. Particularly important is information for stripping by complex, many-electron gases such as N_2 or O_2 since these are the dominant gases in the acceleration and transport regions. Because of their large cross sections, these gases are extremely important contributors to the overall loss, even in ultrahigh vacuum storage rings.

For these reasons, several experimental [3–7] and theoretical [3–5,8–11] studies of electron loss by low-charge-state MeV/u ions have been performed in the past couple of years. Unfortunately, no experimental information for the desired species is available in the tens to hundreds of MeV/u region. Therefore, the purpose of this work is to use available experimental information and extract scaling laws which describe electron loss resulting from collisions with a multi-electron target, i.e., for the process

$$X^{q\pm} + \mathrm{Ar} \rightarrow \sum [X^{(q+n)+} + \mathrm{Ar}^{i+} + (n+i)e^-],$$

$$n \geqslant 1, \quad q \geqslant -1.$$

Here q and n are the initial charge state and number of electrons lost by the projectile and i is the number of target electrons lost. The final state of the target is not monitored, hence the summation over i. Argon was used for the multi-electron target because of the amount of information available.

As will be seen, the empirical scaling formulas we present apply to single- and multiple-electron loss from virtually any projectile. For example, they apply to neutral particles and negative ions, as well as for singly and multiply charged positive ions. They work equally well for light projectiles such as H^-, H^0, and He^+ and for heavy ions such as U^+, Xe^{18+}, or hydrogenlike Au or Pb. They have been applied over an energy range extending from below keV/u to hundreds of MeV/u (to 160 GeV/u in one case).

Several previous investigations relating to scaling laws for electron loss are worth noting. For ions being stripped by light targets, Bohr [12] derived a simple formula based on the free collision approximation. The free collision model is generally associated with small impact parameters where the projectile electron interacts strongly with the target and one can neglect the projectile electron binding energy. Bohr predicted that the stripping cross section σ would be given by

$$\sigma = 4\pi a_o^2 \left(\frac{1}{V}\right)^2 \frac{(Z_2^2 + Z_2)}{Z_1^2}. \quad (1)$$

Here Z_1 and Z_2 are the projectile and target nuclear charges and V is the impact velocity in atomic units. The Z_2^2 term corresponds to interactions between the projectile electron and the target nucleus while the Z_2 term corresponds to interactions between the projectile and target electrons. In the case of medium-heavy targets, the projectile electron interacts with a target that is described by a screened Coulomb potential. In this way Bohr derived

$$\sigma = \pi a_o^2 \left(\frac{1}{V}\right) \frac{Z_2^{2/3}}{Z_1}. \quad (2)$$

Note that in these formulas, the binding energy of the electron being removed is ignored. However for distant collisions, the so-called resonant collision model which accounts for the binding energy of the electron must be used.

Of the numerous theoretical studies that have been performed, except for recent classical trajectory Monte Carlo (CTMC) calculations of Olson *et al.* [3–5,8], all have been based on plane-wave Born calculations. With regard to scaling laws, Shevelko *et al.* have used plane-wave Born approximation calculations [9–11] to calculate stripping cross sections for a variety of projectiles and targets. At high energies, it was predicted that the cross sections should be scaled by multiplying by the projectile ionization potential and dividing by the target *Z*, both raised to the 1.4 power. In addition, the impact energy should be divided by the ionization potential.

Experimentally, most investigations of cross-section scaling have concentrated on target *Z* effects [5,6,13–16] or on the initial projectile charge. For the projectile charge, vastly different dependences were found. The cross sections for highly charged ions are found to decrease extremely fast with increasing projectile charge, e.g., q^{-8-10} in some cases [16–18] but slower $q^{-3-4.4}$ in other cases [19]. In contrast, recent CTMC calculations [3,4] and experiments [4] imply that low-charge heavy ions have a much slower dependence of approximately q^{-1}.

Another way of looking at the charge state dependence is that different charge state ions possess different numbers of electrons that can be removed. Alton *et al.* [20] suggested that the cross sections for single-electron loss should be proportional to the number of electrons in a given subshell N_j since all would have equal probabilities for removal. They also pointed out that most semiempirical formulas for the equilibrium charge states of ions in matter are based on the assumptions that bound electrons having velocities less than the ion velocity will be stripped. Armel and Funkhouser [21] combined an empirical formula for the effective charge of a projectile penetrating a target with the Bohr charge equilibrium condition. For low-charge-state ions, their work predicts that a particular charge state q requires minimum impact velocities that scale as $q/Z_2^{1/3}$. Both studies imply that with increasing impact energies, the number of electrons should increase, and hence the cross-section scaling will change.

Of particular interest for the projects mentioned above is extrapolation to high impact energies. One-electron theories predict a v^{-2} behavior at high energies, which is consistent with Bohr's prediction for interactions with a light target, see Eq. (1) above. In contrast, recent CTMC calculations [3–5,8] predict a slower v^{-1} behavior. This is consistent with what Bohr predicted for medium weight targets, but Bohr obtained his formula using assumptions that are not applicable at high velocities. Experimentally, except for light, few-electron projectiles, the only studies of the velocity dependence for electron loss from fast, heavy ions are by Olson *et al.* [3] for loss from 2 to 9 MeV/u Xe^{18+} ions and by Alonso and Gould [19] for Pb^{q+} ions ($q=36-51$) and Xe^{q+} ions ($q=27-42$) for velocities v/c between 0.099 and 0.134. In both cases, collisions were with N_2. Olson *et al.* found a v^{-1} dependence while Alonso and Gould found $v^{-0.98}$ and $v^{-1.56}$ dependences, respectively.

II. PROCEDURE

Scaling rules for single and multiple electron loss from an arbitrary ion colliding with a many-electron target were deduced in the following manner. First, using experimental information available in the literature, a database was constructed. Then, using selected sets of data from this database the cross-section dependences on impact velocity, number of electrons lost, initial projectile charge, structure or type of projectile ion, etc., were systematically probed. Finally, the dependences that we extracted were combined and adjusted slightly in order to generate a best overall fit to all collision systems and energies.

In extracting the dependences, a few basic principles were kept in mind. First, according to Alton *et al.* [20], the probability of electron loss should increase with the number of projectile electrons available. Second, several studies [3–5,9] indicate that the probability decreases if the electrons are more tightly bound, i.e., with the amount of energy required to remove any particular electron. Third, at low impact energies the threshold velocity for stripping a particular electron will depend on how tightly that electron is bound; more tightly bound electrons will have higher threshold velocities than more loosely bound electrons. Fourth, the probabilities may be larger for "bigger" ions, i.e., there may be a projectile Z or size effect. Lastly, our underlying criteria were that the dependences should be simple in form and should apply for a wide variety of systems and at all energies and not be limited to one-electron systems or restricted energy ranges.

For establishing the database, the primary sources at lower impact energies were the tabulations by Lo and Fite [22] and Dehmel *et al.* [23]. These were supplemented by Refs. [13–20,24–60] and references therein, and unpublished data by one of us (R.D.D.). Recent measurements in the MeV/u regime performed by ourselves and others [3–7,61,62] played an important role in the high-energy regime. If available, tabulated values were used. When only curves were presented, as is the case for the two tabulations, the curves were scanned and digitized at selected impact energies or velocities, the number of points being sufficient for defining the tabulated curve. As a result, over 1400 cross

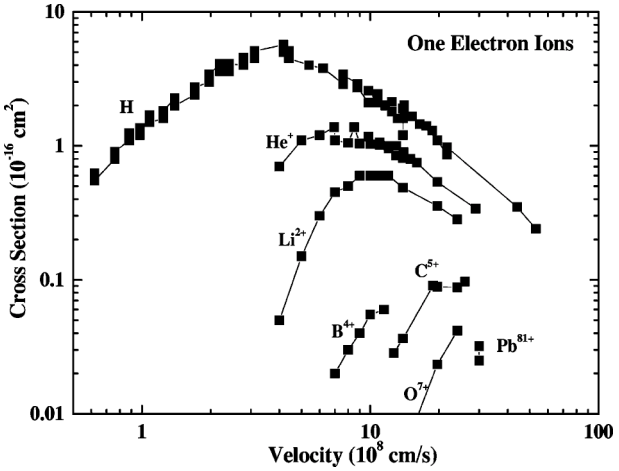

FIG. 1. Measured cross sections for electron loss by hydrogenlike ions. The data are from a variety of sources included in the reference list.

sections were entered into a database. The database includes electron loss from negative ions, neutral projectiles, hydrogenlike ions, singly charged ions, and multiply charged ions. Projectiles included in the database range from hydrogen to uranium, impact energies span the region from a few keV up to hundreds of MeV or even many TeV in one case, and multiple, as well as single, electron loss processes are included. In short, virtually every situation is included.

The database was systematically sorted in terms of initial projectile charge, projectile Z, number of electrons lost, etc., and the selected data were graphed to test for scaling parameters and behaviors. In contrast to previous studies, our extensive database permits detailed testing for each parameter and allows us to examine particular features not readily evident using small sets of data. For example, Fig. 1 shows the absolute cross sections measured for electron loss from several one-electron ions. These data are representative of available information, e.g., for light ions the cross sections have been measured for a wide range of impact velocities and comparison between different projectiles is easy. In contrast, as the projectile becomes heavier, the velocity range of available data becomes smaller and in certain cases only a single impact energy has been investigated. If used alone, the heavier ion data would make it difficult to determine how, or if, the data relate to each other.

But, as Fig. 1 shows, for light ions the stripping cross sections increase to some maximum value and then decrease again. As the projectile becomes heavier and/or the projectile electron becomes more tightly bound, the curves shift downwards and to the right. In addition, for collision velocities less than where the cross section maximizes, with increasing projectile charge the cross sections tend to decrease more rapidly. These three features must be taken into account in order to scale the data to a single curve.

A. Scaling in the high-velocity regime

First let us address the problem of shifting the cross-section maximum to a single velocity, i.e., shifting the curves along the velocity axis. As clearly demonstrated in Fig. 1 for the lighter ions, the stripping cross sections have broad maxima. The maxima are located at velocities roughly equivalent to electron velocities given by $1.5I^{1/2}$, I being the ionization potential of the projectile electron that is removed. Therefore, for one-electron ions scaling the impact velocity by $I^{-1/2}$ shifts the cross-section maxima to a common velocity. This finding is in accordance with the work of Shevelko *et al.* [9].

However, this scaling can also be applied to multiple electron loss if, rather than I, the ionization potential of the most weakly bound projectile electron, I_{sum}, is used. I_{sum} is defined as the sum of the ionization potentials required to remove the required number of electrons in a sequential manner, i.e., the weakest bound electron is removed first, the second weakest next, etc. Thus, for stripping three electrons from a singly charged ion, $I_{sum}=I_1+I_2+I_3$, where $I_{1,2,3}$ are the first, second, and third ionization potentials. We also found that this scaling can be applied to stripping of negative ions. But, for cases where the ionization potential is extremely small, e.g., for single loss from H^-, He^-, Li^-, K^-, and Na^-, we found that an average ionization potential I_{ave} must be used. I_{ave} is defined as the average of the ionization potentials for the negative ion and for the neutral atom. Thus, for these cases, $I_{sum}=I_{ave}$. In the case of double electron loss from negative ions, $I_{sum}=I_{ave}+I_{neutral}$. Our justification for using average values for these cases was simply that it works. Ionization potentials are obtained from Ref. [63] with examples provided in Table I.

Therefore, introducing a scaled projectile velocity defined by

$$V_{sc}(\text{high}) = v\left[\frac{I_H}{I_{sum}}\right]^{1/2} \tag{3}$$

shifts all the cross-section maxima to a single-scaled velocity $V_{sc}(\text{high}) \approx 1.5$ a.u. Here v is the impact velocity in atomic units, I_{sum} is defined above, and I_H is the ionization potential for atomic hydrogen. Please note that v is an intermediate quantity calculated directly from impact energies without applying relativistic corrections.

For shifting the curves vertically, i.e., scaling the cross sections, previous experiments and CTMC theory [3,4] have shown that at a fixed impact velocity and for a fixed ion species, the single and multiple electron loss cross sections scale roughly at I_{sum}^{-1}. By applying the velocity scaling just described and selecting data within a narrow range of scaled velocities, Fig. 2 shows that cross-section scaling as a function of I_{sum} can be applied to an extremely wide range of ions. The dashed curve in Fig. 2 is a fit to the data and, in this case, has a slope of -1. Similar fits performed for many values of V_{sc} between 0.1 and 10 gave an average slope of -1.09 ± 0.18. Hence, multiplying the measured cross sections by $I_{\text{sum}}^{1.09}$ shifts all the data vertically to a common curve.

In addition to this, note that in Fig. 2 the cross sections have been divided by $N_{\text{eff}}^{0.4}$, where N_{eff} is defined

TABLE I. Examples of scaling parameters used. The parentheses in the U^+N_{eff} cell mean that to achieve scaling, the value used for N_{eff} was 1 for single loss and 5 for multiple loss.

Z	Projectile	Electronic configuration	N_{eff}	I_{sum} (eV) 1, 2, etc. loss
1	H^-, D^-	$1s^2$	2	7.18, 20.8 13.6
	H^0,D^0	$1s$	1	
2	He^-	$1s^22s$	3	8.23, 32.8
	He^0	$1s^2$	2	24.59, 79
	He^+	$1s$	1	54.4
3	Li^-	$1s^22s^2$	2	3
	Li^0	$1s^22s$	1	5.39
	Li^+	$1s^2$	2	75.6, 198
	Li^{2+}	$1s$	1	122.5
7	N^0	$[He]2s^22p^3$	3	14.5
	N^+	$[He]2s^22p^2$	4	29.6, 77, 154
	N^{4+}	$[He]2s$	3	98
13	Al^0	$[Ne]3s^23p$	1	5.99
	Al^+	$[Ne]3s^2$	2	18.8, 47
17	Cl^-	$[Ne]3s^23p^6$	6	3.6, 16.6
	Cl^0	$[Ne]3s^23p^5$	5	13
18	Ar^+	$[Ne]3s^23p^5$	7	27.6, 68, 130
	Ar^{6+}	$[Ne]3s^2$	2	124, 268
35	Br^-	$[Ar]3d^{10}4s^24p^6$	6	3.37, 15.2
	Br^0	$[Ar]3d^{10}4s^24p^5$	5	11.8
	Br^{4+}	$[Ar]3d^{10}4s^24p$	3	59.7
	Br^{7+}	$[Ar]3d^{10}$	10	193
54	Xe^+	$[Kr]4d^{10}5s^25p^5$	7	21.2, 53, 93, 175
	Xe^{3+}	$[Kr]4d^{10}5s^25p^3$	5	41.6, 96, 166, 256
	Xe^{11+}	$[Ar]3d^{10}4s^24p^64d^7$	13	245, 521, 797, 828
	Xe^{18+}	$[Ar]3d^{10}4s^24p^6$	18	510, 1064, 1711, 2404, …
79	Au^{52+}	$[Ne]3s^23p^63d^9$	19	3500
92	U^+	$[Rn]5f^36d\ 7s$	1, (5)	11, 30, 59
	U^{27+}	$[Ar]3d^{10}4s^24p^64d^{10}5s^25p^64f^{11}$	47	880, 1800, 2760

as the effective number of projectile electrons that are available for removal. For hydrogenlike projectiles, the number of effective electrons is straightforward. For cases where the difference in binding energies between the shells or subshells is large, again the choice is straightforward. For instance, in the case of C^{3+} and O^{5+} where the electronic configurations are $[He]2s$, the difference in binding energies between the shells is large and N_{eff} only includes the 2s electron. Likewise, for low-charge-state rare-gas ions, when the differences in the binding energies between the subshells is significant, only the outermost p subshell was used. But in many cases the difference in binding energies is not large and the choice of the N_{eff} is rather arbitrary. In these cases, our choice for N_{eff} was based on which best value scaled the data best. Generally, we found that for highly charged but partially stripped projectiles such as U^{27-44+}, N_{eff} must include the outermost shell plus one or more inner shells. Examples of values that were used are provided in Table I.

To determine the power dependence on N_{eff}, cross sections were compared using ions where the number of outermost electrons was fairly certain, e.g., using Ar^+, Ar^{2+}, Ar^{3+}, where $N_{eff}=5,4,3$. These comparisons were made in the vicinity of the cross-section maximum in order to minimize changes associated with impact velocity. Averaging the many cases that were examined yielded the best overall scaling when the cross sections are multiplied by $N_{eff}^{-0.4}$.

Therefore, we define a scaled electron-loss cross section by

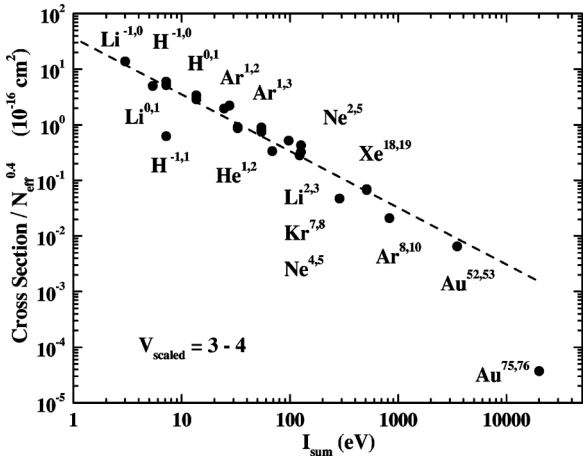

FIG. 2. Cross sections for single and multiple electron loss by various projectiles plotted versus the sum of the ionization potentials obtained assuming sequential removal of the electrons. The superscripts indicate the initial and final projectile charge states. Data are for scaled velocities between 3 and 4. Note that the cross sections are divided by an effective number of projectile electrons. See text for details. The dashed curve is a fit to the data and has a slope of −1.

$$\sigma_{sc} = \sigma \left[\frac{I_{sum}}{I_H} \right]^{1.09} N_{eff}^{-0.4}. \tag{4}$$

To remove large powers of ten, the measured cross sections σ are in units of πa_0^2. This means that the scaled cross sections in the following figures and which can be calculated from the formulas presented later in this paper are also in units of πa_0^2. Plotting σ_{sc} versus V_{sc}(high) compresses a wide range of data to a single curve, as shown in Fig. 3.

B. Scaling in the low-velocity regime

Figure 3 also illustrates that below the cross-section maximum, additional scaling is needed. This is because different

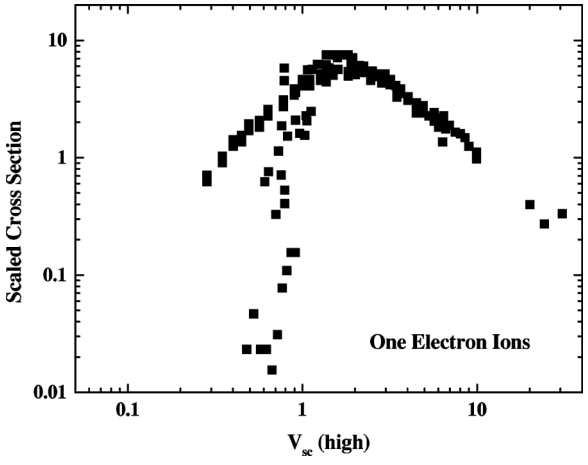

FIG. 3. Scaled cross sections plotted versus scaled velocities for electron loss from hydrogenlike ions. The data are the same as those in Fig. 1. The cross sections have been scaled using Eq. (4) while the impact velocities have been scaled using Eq. (3).

ions or different degrees of stripping will have different impact energy (velocity) thresholds since different amounts of energy are required to remove the projectile electrons. But, as seen in Fig. 3, although the threshold velocities may change, all the cross sections maximize at nearly the same scaled velocity and all have the same maximum cross section. Thus, for impact velocities below the cross-section maximum, the slope of the curves are different and a more complex formula is required to scale the impact velocities.

Regarding the velocity where the scaled cross sections maximize, using a wider variety of systems than shown in Fig. 3 demonstrated that the curves maximize at slightly lower velocities for heavier ions and at slightly higher velocities for projectiles having higher initial charge states. Accounting for these effects was necessary in order to minimize the overall spread in the scaled low-velocity data.

Numerous attempts were made to find a simple scaling that would account for threshold effects as well as for shifts associated with projectile mass and initial charge. The best overall compression of data to a single curve was obtained using the following formulas to scale the collision velocities between zero and the cross section maximum:

$$\langle V_{sc} \rangle = v \left[n \frac{I_H}{I_{sum}} \right]^{1/2} q_{in}^{-0.15} \tag{5}$$

and

$$V_{sc}(\text{low}) = 1.5^{[1-(I_{sum}/I_H)^{0.3}]} \langle V_{sc} \rangle^{[I_{sum}/I_H]^{0.3}} q_{in}^{-0.25} Z^{0.5 \log_{10}(I_{sum}/I_H)}. \tag{6}$$

In Eq. (5), n is the principal quantum number of the outermost projectile electron and q_{in} is the initial projectile charge state. For negative ions and neutral projectiles, q_{in} was defined to be +1. $\langle V_{sc} \rangle$ is an intermediate scaled velocity used in Eq. (6). In Eq. (6), Z is the projectile nuclear charge and the value of 1.5 corresponds to the scaled velocity where the cross sections reach their maximum value.

Effectively, Eq. (5) shifts the position of the maximum cross section to a common value with n and q_{in} shifting more or less depending on the "size" of the projectile or its initial charge state. Equation (6) adjusts the slope of the curves on a log-log scale by "stretching" the scaled velocities in the low-velocity regime. As shown in Fig. 4, for electron loss by one-electron ions, using this velocity scaling greatly improves the scaling below the cross-section maximum although the F^{8+} data are still slightly offset.

III. RESULTS

The best overall compression of data to a single universal curve was achieved by scaling the cross sections according to Eq. (4) and the impact velocities according to Eq. (3) in the high-velocity regime or by Eqs. (5) and (6) in the low-velocity regime. The high- and low-velocity regimes correspond to scaled velocities greater than/less than 1.5, i.e., to the right/left of the cross-section maximum. The data were binned in narrow scaled velocity intervals and average val-

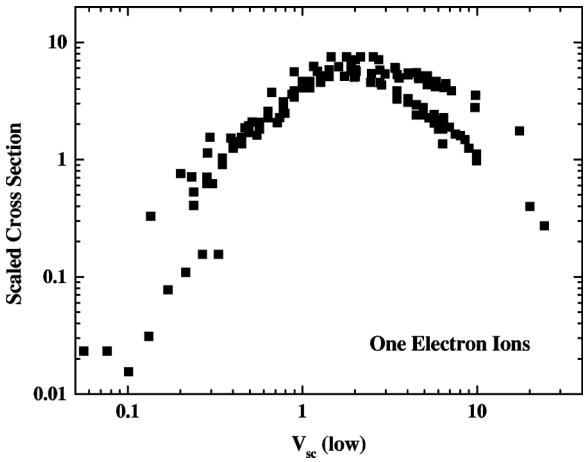

FIG. 4. Scaled cross sections plotted versus scaled velocities for electron loss from hydrogenlike ions. The data are the same as those in Figs. 1 and 3. The cross sections have been scaled using Eq. (4) while the impact velocities have been scaled using Eqs. (5) and (6).

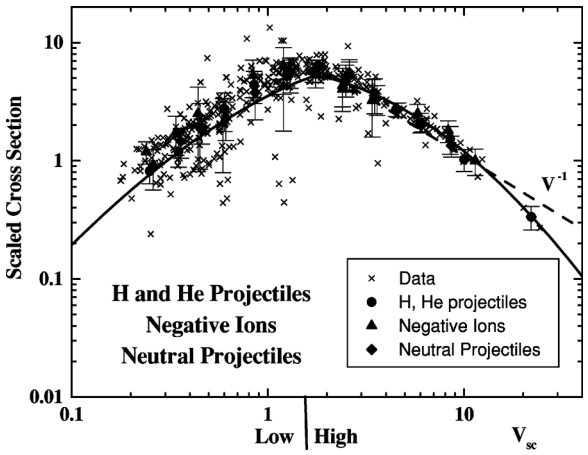

FIG. 5. (Color online) Scaled cross sections for single and multiple electron loss by H and He projectiles, negative ions, and neutral particles in collisions with argon. The crosses are the individual scaled data while the solid symbols and error bars show average values within narrow velocity bins. The cross sections are scaled according to Eq. (4). To the right of the cross-section maxima indicated by the division on the velocity axis, the collision velocities are scaled according to Eq. (3); to the left they are scaled according to Eqs. (5) and (6). The solid and dashed curves are our average second-order polynomial and linear fits to the data.

ues plus standard deviations were calculated. These were fitted with second-order polynomials, weighted with respect to the magnitude of the error bars. Fitting parameters for individual data sets as well as for the entire data set are given in Table II. From these fitting parameters, scaled cross sections, in units of πa_0^2, for single or multiple electron loss from an arbitrary ion interacting with an argon target at an arbitrary scaled velocity between 0.2 and 30 a.u. can be determined using the following equation:

$$\sigma_{sc} = 10^{A} V_{sc} 10^{C[\ln(V_{sc})]^2}. \tag{7}$$

Below the cross-section maximum, specifically for $0.2 < V_{sc} < 2$, Eqs. (5) and (6) are used to convert between scaled and impact velocities. Above the cross-section maximum, i.e., for $1 < V_{sc} < 30$, Eq. (3) is used to convert between scaled and impact velocities. Then the fitting parameters in Table II and Eqs. (7) and (4) can be used to predict the cross sections for single or multiple electron removal.

Because of our interest in extrapolation to higher energies, we also fitted the data having scaled velocities greater than 2 with a first-order polynomial. The result was $\sigma = 10^{1.05} V_{sc}^{-1}$ with both powers having uncertainties of approximately 10%. Whether the linear fit, the average polynomial fit, or the fit for a particular subgroup of ions is used is left to the discretion of the user. Below the cross-section maximum, the individual polynomial fits agree with the average fit within ± a factor of 2–3 at $V_{sc} = 0.2$ and within =30% at $V_{sc} = 1$. Above the cross-section maximum, all the polynomial fits agree within ±20% over the entire velocity range. In the scaled velocity range between 2 and 20, the polynomial and the linear fits agree within 30%.

In Figs. 5–8 we present our scaled electron-loss cross sections as a function of our scaled impact velocities for all available argon target data that we were able to find in the literature. The figures show the individual scaled cross sections (crosses) along with average values calculated within narrow velocity ranges (symbols plus error bars) and solid

TABLE II. Second-order polynomial fitting parameters used in Eq. (7) for various sets of data. The top row shows the range of scaled velocities where these parameters apply; the last column gives the highest scaled velocity where data exist for a particular subgroup.

	$0.2 < V_{sc}(\text{low}) < 2$			$1 < V_{sc}(\text{high}) < 30$			
Coefficient	A	B	C	A	B	C	Max V_{sc} of data
H and He particles	0.598	0.762	−0.644	0.828	−0.255	−0.534	~10
Negative ions	0.617	0.538	−0.547	0.700	0.227	−0.821	~10
Neutral projectiles	0.608	0.830	−0.478	0.880	−0.338	−0.500	~20
Singly charged ions	0.353	1.176	−0.498	0.687	0.447	−0.975	~7
One-electron ions	0.587	1.083	−0.441	0.961	−0.549	−0.363	~20
Single-electron loss	0.472	0.876	−0.107	0.580	0.293	−0.806	~20
Average fit	0.547	0.849	−0.413	0.780	−0.044	−0.659	

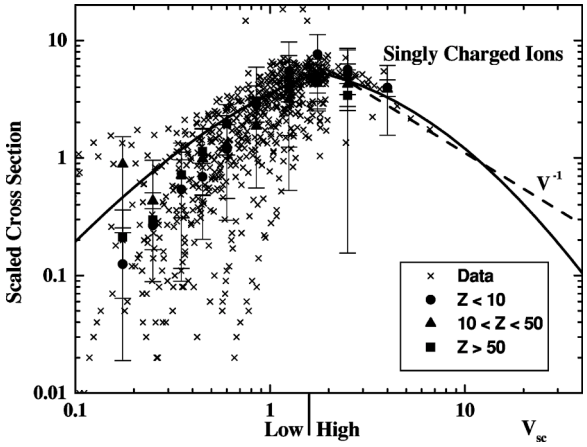

FIG. 6. (Color online) Scaled cross sections for single and multiple electron loss by singly charged positive ions colliding with argon. Symbols and curves are as described in Fig. 5 where averages have been taken for selected ranges of projectile *Z*.

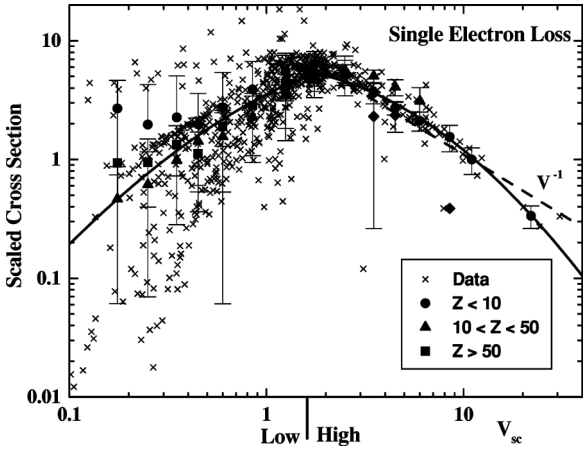

FIG. 8. (Color online) Scaled cross sections for single electron loss by singly charged positive ions colliding with argon. Symbols and curves are as described in Fig. 5 where averages have been taken for selected ranges of projectile *Z*.

curves that are our average second-order polynomial fits. They also show our linear, high energy fits (the dashed curves).

A. H and He projectiles; negative ions; neutral projectiles

Figure 5 presents data for electron loss from H and He projectiles, from negative ions, and from neutral projectiles. Note that there is overlap between these groups, i.e., H projectiles include H^- and H^0, which are also included in the negative-ion and neutral-particle categories. Also note than the negative ions and neutral particles range from light species such as H and He to heavy species such as Br and I. As mentioned previously, for negative ions it was found that scaling could only be achieved by using an average ionization potential for situations where the projectile electron was bound by less than 1 eV. In addition, we found that the scaled cross sections for double loss from H^-, He^-, and He^0 were uniformly a factor of 2 smaller than the majority of the data. Therefore, for calculating our average values and fitting the data, we have arbitrarily multiplied these double-loss data by a factor of 2. This represents the only situation where the scaled data were adjusted after applying our scaling formulas.

As seen, below the cross-section maximum the vast majority of the scaled data falls within a factor of 2 of the solid curve, our recommended best fit using the entire database of experimental cross sections. Above the maximum, fewer data are available and the scaled data agree within ±25% of the solid curve. The scaling is seen to apply equally well for light projectiles, negative ions, or neutral projectiles. The dashed curve is the linear fit to the high scaled velocity data. The data imply that above $V_{sc} \sim 10$, the second-order polynomial is superior and that our linear fit would be in better agreement if it were shifted upwards by approximately 20%.

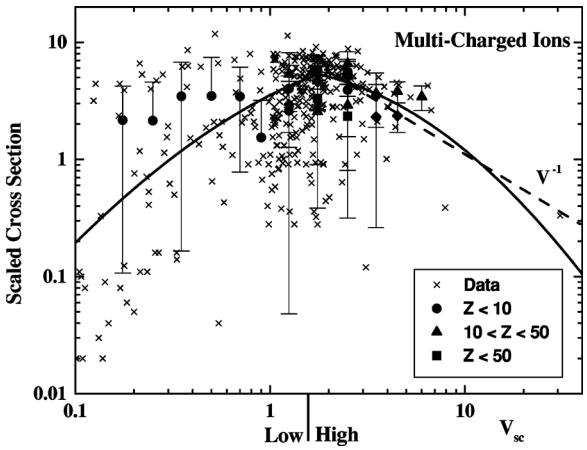

FIG. 7. (Color online) Scaled cross sections for single and multiple electron loss by multiply charged positive ions colliding with argon. Symbols and curves are as described in Fig. 5 with averages shown for selected ranges of projectile *Z*.

B. Singly charged ions

Figure 6 presents all available data for singly charged ions being stripped by argon. These ions range from He^+ to U^+. Therefore, in calculating average values we have grouped the data into light, medium weight, and heavy-ion categories. As seen, the majority of the singly charged ion data fall within the low scaled velocity regime. Although there is scatter in the scaled data, the average values are in excellent agreement with each other and our average curve, independent of projectile *Z*. At very low velocities, these average values fall below our recommended fit. Finally, please note that few data above the scaled cross-section maximum are available and that for heavy ions no data exist for scaled velocities greater than $V_{sc} \sim 3$. Therefore, whether our linear or polynomial extrapolation to higher velocities is better cannot be determined.

C. Multicharged ions

Figure 7 presents data for single and multiple electron loss from multiply charged ions. Although the vast majority

of these data are for collisions with an argon target, we have included stripping cross sections for Kr^{7+}-, $Xe^{11+,18+}$-, $Au^{52+,75+}$-, and Pb^{81+}-N_2 collisions in order to supplement the high-energy portion of our database. Including these data is justified by experiments performed in the MeV/u range [4,7,62] which yield similar stripping cross sections for collisions with argon and molecular nitrogen targets.

The importance of these multicharged ion data is that the traditional approach for investigating processes at high collision velocities is to use highly charged ions. However, as seen, scaling the impact velocities by $I_{sum}^{-1/2}$ means that the majority of the data are shifted to the vicinity of the cross-section maximum and do not help in extrapolating to high velocities or in determining which velocity dependence is correct. There is considerable scatter in the scaled data. But the reader is reminded that these data range from single- to many-electron loss from ions ranging from doubly charged light ions to highly stripped heavy ions and for energies ranging from a few keV/u to many tens or hundreds of MeV/u. This means that for some of the data both the cross sections and the velocities have been scaled by factors of 100–1000 or more. Because of the scatter, no polynomial fit to the data was made. But the average values are seen to generally agree within a factor of 2 of the solid curve.

D. Single electron loss

Figure 8 presents data for single electron loss from negative ions, neutral particles, and singly or multiply charged positive ions. In the high-velocity regime and near the cross-section maximum, all the data fall within ±50% of our recommended value. For lower impact velocities the scatter is larger, roughly ± a factor of 2–3. Averages for narrow velocity slices are shown for light, intermediate weight, and heavy ions. Again our linear fit is in good agreement for scaled velocities less than 10. As before, the linear fit is roughly 20% below the data.

E. Velocity dependences and cross-section predictions

Our goals when initiating this work were to (a) establish scaling rules for electron loss from an arbitrary ion induced by collisions with a many-electron target and (b) to predict stripping cross sections at high energies for low-charge-state heavy ions where no experimental information exists. We have shown that, generally within a factor of 2, cross sections for stripping one or more electrons from virtually any projectile at any impact energy agree with our universal fit. Therefore, within a factor of 2 we expect to be able to predict cross sections using the fitting parameters given in Table II and the equations given above. For extrapolation purposes, our fits show that below the cross-section maximum the scaled cross sections increase roughly linearly with the scaled impact velocity V_{sc}. Above the cross-section maximum, our second-order polynomial fits decrease roughly as V_{sc}^{-1} up to $V_{sc}\sim 10$, and then approximately as V_{sc}^{-2}. A linear fit to all data above $V_{sc}=2$ had a V_{sc}^{-1} dependence.

With regard to the Heavy Ion Fusion project in the USA and the Accelerator Upgrade at Darmstadt, the interest is in accelerating intense beams of low-charge-state, heavy ions to

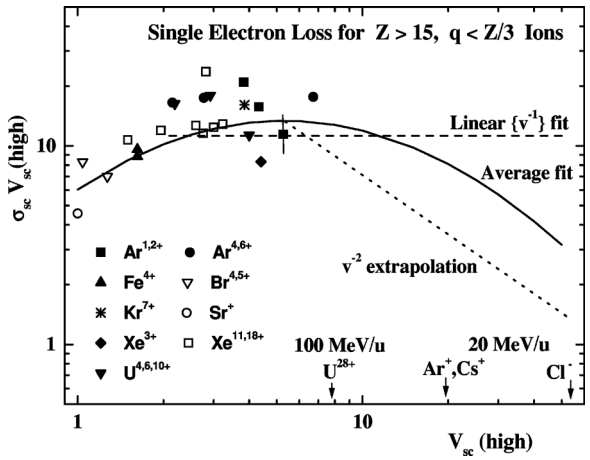

FIG. 9. (Color online) Scaled cross sections for single electron loss by fast, heavy, low-charge-state positive ions colliding with argon. Symbols show all known data for ions with $Z>15$ and initial charge state $q<Z/3$; $Ar^{1,2+}$, Xe^{3+}, Ref. [4]; $Ar^{4,6+}$, Refs. [7,45]; Fe^{4+}, Ref. [15]; $Br^{4,5+}$, Ref. [30]; Kr^{7+}, Xe^{11+}, Refs. [6,7]; Sr^{+}, Ref. [22]; Xe^{18+}, Ref. [3]; $U^{4,6,10+}$, Ref. [62]. The solid curve is our average second-order polynomial fit, the dashed curve is a linear fit to all high scaled velocity data and has a velocity dependence of v^{-1}. The dotted curve is a v^{-2} extrapolation from the data shown in this figure. Indicated on the x axis are scaled velocities for ions of interest to the USA heavy-ion fusion program and the accelerator upgrade at GSI-Darmstadt.

tens or hundreds of MeV/u respectively. In Fig. 9 we show all available data for single electron loss from heavy ($Z>15$), low-charge-state ($q_{\rm in}/Z<1/3$) ions and compare these data to our overall polynomial and linear fits (the solid and dashed curves). In making this comparison, we plot $\sigma_{sc}V_{sc}$(high) versus V_{sc}(high). Thus, a v^{-1} dependence will be a horizontal line. The arrows at the bottom axis indicate scaled velocities for high-energy, low-charge-state heavy ions of interest.

Plotted in this manner, the measured cross sections monotonically increase until $V_{sc}\sim 2$. For $V_{sc}=2-7$ they scatter around an average value of 15 ± 4. The agreement between the data and our fits is on the order of the typical uncertainty in the measurements, as indicated by the error bar on the data point at $V_{sc}\sim 5$. Also shown in Fig. 9 is a dotted curve representing a v^{-2} extrapolation beginning at the last data point. The reader is reminded that a v^{-2} dependence is predicted by one-electron theories and that according to Eq. (1), the scaled and unscaled impact velocities are proportional, so they have the same velocity dependences.

These fits and extrapolations predict the following. The cross sections for one electron loss from a 20 MeV/u singly charged heavy ion (Ar^{+} or Cs^{+}, where $V_{sc}\sim 20$ and $N_{eff}=5$ and 6, respectively), i.e., possible candidates for the USA Heavy Ion Fusion program, are approximately 4×10^{-17} cm^2 using our average polynomial fit, $\sim 5\times 10^{-17}$ cm^2 assuming our linear (v^{-1}) fit, and 1.6×10^{-18} cm^2 assuming the v^{-2} extrapolation shown in Fig. 9.

For Heavy Ion Fusion, it has also been suggested that a heavy negative ion could be used. Our study would predict

the following cross sections for a 20 MeV/u Cl^- ion (where $V_{sc} \sim 54$ and $N_{eff}=6$); $\sim 4 \times 10^{-17}$ cm^2 using our average polynomial fit, $\sim 1.5 \times 10^{-16}$ cm^2 assuming our linear fit, and 1.9×10^{-17}cm^2 assuming the v^{-2} extrapolation. In the case of the accelerator upgrade at GSI-Darmstadt, a possible candidate for studies is a 100 MeV/u U^{28+} ion (where $V_{sc} \sim 8$ and $N_{eff}=46$). Existing data and our study predict that the cross section for one electron loss would be approximately 7×10^{-18} cm^2 with little uncertainty introduced by extrapolating outside the existing data regime. This is in excellent agreement with CTMC calculations [64].

Regarding these estimates, we would like to emphasize several points. First, although our fits are based on a large amount of existing data, we have extrapolated far outside the available information for heavy ions, particularly in the cases of Ar^+, Cs^+, and Cl^-. Second, as seen in Figs. 5–8, most individual measurements agree within approximately a factor of 2 of the fitted curve but in certain cases much larger deviations occur. Third, based upon existing data, there is no indication that the cross sections should scale as v^{-2} for $V_{sc} < 10$. Therefore, we consider the smaller cross sections quoted above using the v^{-2} extrapolation beginning at $V_{sc} \sim 5$ to be too small and highly unlikely. Fourth, a linear fit to all data above scaled velocity 2 yielded a $v^{-1\pm0.1}$ impact velocity dependence. This is consistent with CTMC predictions for electron loss from many-electron ions. Using our v^{-1} fit to predict stripping of 20 MeV/u Ar^+ ions yields single electron loss cross sections that agree reasonably well with CTMC calculations [4]. The agreement is even better if the linear fit were made using only the low-charge-state heavy-ion data shown in Fig. 9. Thus, in extrapolating to scaled velocities larger than ~ 10, the v^{-1} curve (linear fit) shown in Fig. 9 may be more accurate for projectiles carrying many electrons whereas for few-electron projectiles our polynomial fit may be more appropriate. Finally, to avoid confusion the reader is reminded that the cross sections predicted in the previous paragraph are for single electron loss. According to several recent studies [4,62], total loss cross sections from these heavy singly charged ions are roughly a factor of 2 larger. Or, total loss cross sections could be estimated by using Fig. 9 to extract double, triple, and higher electron-loss cross sections for the desired systems and summing the results.

IV. SUMMARY

To summarize, scaling behaviors for electron loss resulting from collisions with argon atoms have been studied using experimental data measured for a wide variety of projectiles and impact velocities. It was found that the cross sections scale roughly as I_{sum}^{-1} and $N_{eff}^{0.4}$, where I_{sum} is the sum of the ionization potentials assuming sequential removal of the weakest, next weakest, etc. bound electrons and N_{eff} is the effective number of projectile electrons available. In the high-velocity regime, the impact velocities scale as $I_{sum}^{-0.5}$; in the low-velocity regime, the velocity scaling is more complex since it must account for different threshold energies and other effects. Using this large data set which covers virtually any possible projectile and velocity, universal cross-section scaling formulas have been presented. On the average, for scaled velocities between approximately 0.5 and 20, the formulas are considered to have predictive capabilities with accuracy within a factor of 2. At very low energies, threshold effects make them less reliable. At very high energies and particularly for projectiles possessing weakly bound electrons, extrapolations outside the existing data set are required, so the results become inherently less and less accurate.

For extrapolation to high energies, it was shown that the best fit to all the high-energy data had roughly a V_{sc}^{-1} dependence for scaled velocities up to approximately 10 followed by a V_{sc}^{-2} dependence at higher scaled velocities. Using our fits and a v^{-2} extrapolation, cross sections were predicted for particular systems of interest in the USA and Germany. Available information indicate that the v^{-2} extrapolation underestimates the cross sections in this particular case and that for low-charge-state heavy ions, the linear fit may be more appropriate. Finally, we note that although our work is based on stripping by argon atoms the same formulas should apply for interactions with molecular nitrogen because both targets yield similar stripping cross sections.

ACKNOWLEDGMENTS

This work was supported by the U.S. Department of Energy, Grant No. ER54578. A.C.F.S. is grateful for support obtained from CNPq (Brazil).

[1] See the Lawrence Berkeley Laboratory Heavy Ion Fusion homepage website, http:/www-hifar.lbl.gov/HIFhomepage/hithome.html

[2] See the GSI future project website, http:/www-new.gsi.de/zukunftsprojekt/index_e.html

[3] R. E. Olson, R. L. Watson, V. Horvat, and K. E. Zaharakis, J. Phys. B **35**, 1893 (2002).

[4] R. D. DuBois, A. C. F. Santos, R. E. Olson, Th. Stöhlker, F. Bosch, A. Bräuning-Demian, A. Gumberidze, S. Hagmann, C. Kozhuharov, R. Mann, A. Oršić Muthig, U. Spillmann, S. Tachenov, W. Barth, L. Dahl, B. Franzke, J. Glatz, L. Gröning, S. Richter, D. Wilms, A. Krämer, K. Ullmann, and O. Jagutzki, Phys. Rev. A **68**, 042701 (2003).

[5] R. L. Watson, Y. Peng, V. Horvat, G. J. Kim, and R. E. Olson, Phys. Rev. A **67**, 022706 (2003).

[6] D. Mueller, L. Grisham, I. Kaganovich, R. L. Watson, V. Horvat, E. Zaharakis, and M. S. Armel, Phys. Plasmas **8**, 1753 (2001).

[7] D. Mueller, L. Grisham, I. Kaganovich, R. L. Watson, V. Horvat, K. E. Zaharakis, and Y. Peng, Princeton Plasma Physics

Laboratory Report No. PPPL-3713, 2002 (unpublished).
[8] R. E. Olson, Nucl. Instrum. Methods Phys. Res. A **464**, 93 (2001).
[9] V. P. Shevelko, I. Yu. Tolstikhina, and Th. Stöhlker, Nucl. Instrum. Methods Phys. Res. B **184**, 295 (2001).
[10] V. P. Shevelko, D. Böhne, and Th. Stöhlker, Nucl. Instrum. Methods Phys. Res. A **415**, 609 (1998).
[11] V. P. Shevelko, O. Brînzanescu, W. Jacoby, M. Rau, and Th. Stöhlker, Hyperfine Interact. **114**, 289 (1998).
[12] N. Bohr, Mat. Fys. Medd. K. Dan. Vidensk. Selsk. **18**, 1 (1948).
[13] I. S. Dmitriev, N. F. Vorob'ev, Zh. N. Konovalova, V. S. Nikolaev, V. N. Nozozhilova, Ya. A. Teplova, and Yu. A. Fainberg, Zh. Eksp. Teor. Fiz. **84**, 1987 (1983) [Sov. Phys. JETP **57**, 1157 (1983)].
[14] S. A. Boman, E. M. Bernstein, and J. A. Tanis, Phys. Rev. A **39**, 4423 (1989).
[15] H. Knudsen, C. D. Moak, C. M. Jones, P. D. Miller, R. O. Sayer, G. D. Alton, and L. B. Bridwell, Phys. Rev. A **19**, 1029 (1979).
[16] W. G. Graham, K. H. Berkner, R. V. Pyle, A. S. Schlachter, J. W. Stearns, and J. A. Tanis, Phys. Rev. A **30**, 722 (1984).
[17] K. H. Berkner, W. G. Graham, R. V. Pyle, A. S. Schlachter, and J. W. Stearns, Phys. Rev. A **23**, 2891 (1981).
[18] K. H. Berkner, W. G. Graham, R. V. Pyle, A. S. Schlachter, and J. W. Stearns, Phys. Lett. **62A**, 407 (1977).
[19] J. Alonso and H. Gould, Phys. Rev. A **26**, 1134 (1982).
[20] G. Alton, L. B. Bridwell, M. Lucas, C. D. Moak, P. D. Miller, C. M. Jones, Q. C. Kessel, A. A. Antar, and M. D. Brown, Phys. Rev. A **23**, 1073 (1981).
[21] M. S. Armel and M. S. Funkhouser, Phys. Rev. A **64**, 064502 (2001).
[22] H. H. Lo and W. L. Fite, At. Data **1**, 305 (1970).
[23] R. C. Dehmel, H. K. Chau, and H. H. Fleischmann, At. Data **5**, 231 (1973).
[24] I. S. Dmitriev, V. S. Nikolaev, L. N. Fateeva, and Ya. A. Teplova, Zh. Eksp. Teor. Fiz. **42**, 16 (1962) [Sov. Phys. JETP **15**, 11 (1962)].
[25] I. S. Dmitriev, V. S. Nikolaev, L. N. Fateeva, and Ya. A. Teplova, Zh. Eksp. Teor. Fiz. **43**, 341 (1962) [Sov. Phys. JETP **16**, 259 (1963)].
[26] R. Smutythe and J. W. Toevs, Phys. Rev. **139**, A15 (1965).
[27] L. M. Welsh, K. H. Berkner, S. N. Kaplan, and R. V. Pyle, Phys. Rev. **158**, 85 (1967).
[28] J. F. Williams, Phys. Rev. **154**, 9 (1967).
[29] J. K. Layton, R. F. Stebbings, R. T. Brackmann, W. L. Fite, W. R. Ott, C. E. Carlston, A. R. Comeaux, G. D. Magnuson, and P. Mahadevan, Phys. Rev. **161**, 73 (1967).
[30] S. Datz, H. O. Lutz, L. B. Bridwell, and C. D. Moak, Phys. Rev. A **2**, 430 (1970).
[31] F. R. Simpson and H. B. Gilbody, J. Phys. B **5**, 1959 (1972).
[32] H.-D. Betz, Rev. Mod. Phys. **44**, 465 (1972).
[33] S. M. Ferguson, J. R. Macdonald, T. Chiao, L. D. Ellsworth, and S. A. Savoy, Phys. Rev. A **8**, 2417 (1973).
[34] J. Heinemeier, P. Hvelplund, and F. P. Simpson, J. Phys. B **8**, 1880 (1975); **9**, 2669 (1976).
[35] W. Erb and B. Franzke, GSI Report No. GSI-J-1-78 119, 1978 (unpublished); GSI-P-7-78, 1978 (unpublished).
[36] B. Franzke, IEEE Report No. NS-28, 1981 (unpublished).
[37] C. J. Anderson, R. J. Girnius, A. M. Howald, and L. W. Anderson, Phys. Rev. A **22**, 822 (1980).
[38] W. J. Lichtenberg, K. Bethge, and H. Schmidt-Böcking, J. Phys. B **13**, 343 (1980).
[39] H. Knudsen, L. H. Andersen, H. K. Haugen, and P. Hvelplund, Phys. Scr. **26**, 132 (1982).
[40] Y. Nakai, A. Kikuchi, T. Shirai, and M. Sataka, JAERI-M Report No. 84-069, 1984 (unpublished).
[41] D. P. Almeida, N. V. de Castro Faria, F. L. Freire, Jr., E. C. Montenegro, and A. G. de Pinho, Phys. Rev. A **36**, 16 (1987).
[42] R. Anholt, X.-Y. Xu, Ch. Stoller, J. D. Molitoris, W. E. Meyerhof, B. S. Rude, and R. J. McDonald, Phys. Rev. A **37**, 1105 (1988).
[43] B. Hird, F. Rahman, and M. W. Orakzai, Phys. Rev. A **37**, 4620 (1988).
[44] B. Hird, F. Rahman, and M. W. Orakzai, Can. J. Phys. **66**, 972 (1988).
[45] T. Tonuma, H. Kumagai, T. Matsuo, and H. Tawara, Phys. Rev. A **40**, 6238 (1989).
[46] R. D. DuBois, Phys. Rev. A **39**, 4440 (1989).
[47] B. Hird, M. W. Orakzai, and F. Rahman, Phys. Rev. A **39**, 5010 (1989).
[48] B. Hird, B. M. Elrick, H. Lacasse, J. H. LaCasse, and P. Tume, Phys. Rev. A **41**, 5217 (1990).
[49] O. Heber, R. L. Watson, G. Sampoll, and B. B. Bandong, Phys. Rev. A **42**, 6466 (1990).
[50] R. W. McCullough, M. B. Shah, M. Lennon, and H. B. Gilbody, J. Phys. B **15**, 791 (1982).
[51] H.-P. Hülskötter, B. Feinberg, W. E. Meyerhof, A. Belkacem, J. R. Alonso, L. Blumenfeld, E. A. Dillard, H. Gould, N. Guardala, G. F. Krebs, M. A. McMahan, M. E. Rhoades-Brown, B. S. Rude, J. Schweppe, D. W. Spooner, K. Street, P. Thieberger, and H. E. Wegner, Phys. Rev. A **44**, 1712 (1991).
[52] H. Atan, W. Steckekmacher, and M. W. Lucas, J. Phys. B **24**, 2559 (1991).
[53] M. M. Sant'Anna, W. S. Melo, A. C.F. Santos, G. M. Sigaud, and E. C. Montenegro, Nucl. Instrum. Methods Phys. Res. B **99**, 46 (1995).
[54] O. Heber, G. Sampoll, B. B. Bandong, R. J. Maurer, R. L. Watson, I. Ben-Itzhak, J. M. Sanders, J. L. Shinpaugh, and P. Richard, Phys. Rev. A **52**, 4578 (1995).
[55] W. S. Melo, M. M. Sant'Anna, A. C. F. Santos, G. M. Sigaud, and E. C. Montenegro, Phys. Rev. A **60**, 1124 (1999).
[56] H. Martinez, A. Amaya-Tapia, and J. M. Hernández, J. Phys. B **33**, 1935 (2000).
[57] H. F. Krause, C. R. Vane, S. Datz, P. Grafström, H. Knudsen, U. Mikkelsen, C. Scheidenberger, R. H. Schuch, and Z. Vilakazi, Phys. Rev. A **63**, 032711 (2001).
[58] P. G. Reyes, F. Castilho, and H. Martinez, J. Phys. B **34**, 1485 (2001).
[59] E. Marquina, A. Amaya-Tapia, R. Hernández-Lamonedam, and H. Maratínez, J. Phys. B **34**, 3751 (2001).
[60] P. G. Reyes, F. Castilho, and H. Martínez, J. Phys. B **34**, 1485 (2001).
[61] R. D. DuBois, A. C. F. Santos, V. Horvat, Y. Peng, and R. L. Watson Phys. Rev. A **68**, 042701 (2003).
[62] R. D. DuBois, A. C. F. Santos, Th. Stöhlker, F. Bosch, A. Bräuning-Demian, A. Gumberidze, S. Hagmann, C. Kozhuharov, R. Mann, A. Oršić Muthig, U. Spillmann, S. Tachenov, W. Barth, L. Dahl, B. Franzke, J. Glatz, L. Gröning, S. Richter,

D. Wilms, A. Krämer, K. Ullmann, O. Jagutzki, and R. E. Olson (unpublished).

[63] T. A. Carlson, C. W. Nestor, Jr., N. Wasserman, and J. D. McDowell, At. Data **2**, 63 (1970).

[64] R. E. Olson, R. L. Watson, V. Horvat, K. E. Zaharakis, and Th. Stöhlker, in *Applications of Accelerators in Research and Industry*, edited by J. L. Duggan and I. L. Morgan, AIP Conf. Proc. No. 680 (AIP, Melville, NY, 2003), p. 184.